Turkish J. Eng. Env. Sci.
31 (2007) , 323 – 331.

Influence of Degradation Gases on Laminar Flames from Forest Fuels

V. TIHAY, A. SIMEONI, P. A. SANTONI
SPE–UMR 6134 CNRS, University of Corsica, Campus Grossetti,
BP 52, 20250 Corte-FRANCE
e-mail: tihay@univ-corse.fr
J. P. GARO and J. P. VANTELON
LCD – UPR 9028 CNRS, ENSMA, University of Poitiers, 1 avenue Clément Ader,
Téléport 2 – BP 40109, 86961 Futuroscope Chasseneuil Cedex-FRANCE

Received 16.11.2006

Abstract

The aim of this work is to identify the parameters influencing the flame behavior. Three different species (*Pinus pinaster*, *Pinus halepensis* and *Erica arborea*) involved in forest fire were crushed to decrease the geometric effects on their combustion. The flaming behavior is studied experimentally from unsteady, axisymmetric, non-premixed laminar flames. The distribution of temperature, the flame geometry, the mass loss as well as the gases released by the fuels are measured. This study confirms the role of the mass burning rate of fuels on the flame dynamics. However, this work highlights a second influence for laminar flames: the composition of degradation gases. It affects the flame geometry and changes the combustion kinetics in the reaction zone.

Key words: Forest fire, degradation gas influence

Introduction

Forest fire is a complex phenomenon in which the levels of description cover a huge range, from the details of kinetics of combustion and thermal degradation of fuels, up to the physical-chemistry characterization of flames and vegetation cover as a fuel. Experiments at laboratory scale investigate the burning of vegetative fuels by the way of different kinds of studies. The thermal degradation processes of the plant species are investigated by thermal analysis and calorimetric studies (Philpot, 1970; Ghetti et al., 1996; Klose et al., 2000). The static combustion of forest fuel (Dupuy et al., 2003; Saâdaoui et al., 2007) records and compares the mass loss, the flame geometry and the temperature distribution. The experiments of fire propagation in pine needle beds (Rothermel and Anderson, 1998; Viegas, 1998; Dupuy, 1995; Mendes-Lopes et al., 2003) are focused on the determination of the rate of spread following different conditions (wind, slope, fuel characteristics...). The last aspects concern the study of the composition of degradation gases released by the forest fuel (Klose et al., 2000; Grishin et al., 1985). However, up to now, no studies allow classifying the parameters involved in fire behavior in order to model their influence. Our study is motivated by this observation and aims to improve the knowledge on this domain. As the geometry of a forest fuel plays a dominant role in its combustion, we choose to free us from this parameter in order to focus on other elements. The different species are crushed and sieved to obtain samples with a same mass and particle size. The flaming behavior is studied experimentally from unsteady, axisymmetric, non-premixed laminar flames resulting from the sample burning. During the set of experiments, the distribution of temperature along the flame, the flame geometry, the mass loss as well as the gases re-

leased by the degradation of the fuels are measured. The experimental procedures are described in the following section. And then, the experimental results are presented and discussed.

Experimental Devices

We studied the burning of three Mediterranean fuels: *Pinus pinaster*, *Pinus halepensis* and *Erica arborea* involved in wildland fires. They were collected in winter during a period of hydrous stress for vegetation. Before experiments, the plants were oven dried at 333 K for 24 hours and then they were crushed and sieved to a particle size between 0.6 and 0.8 mm. The mean surface-to-volume ratio of the particles was obtained thanks to a granulometric analysis. A sample of each species was treated by image processing using a high resolution scanner. It provided the mean length and the width of the particles. By assuming that the shape of the particles was a cylinder, the mean surface-to-volume ratios of the samples are 6494, 6083 and 6755 m^{-1} respectively for *Pinus pinaster*, *Pinus halepensis* and *Erica arborea*. The geometry of the fuel sample is also equivalent for the three species. The moisture content due to self-rehydration was less than 2 % for all the samples before each burning. The ultimate analysis of each species performed by the Service Central d'Analyse (CNRS, France) is presented in Table 1.

Table 1. Ultimate analysis for the three fuels.

	Elements (Wt. %)				
	C	H	O	N	Ash
Pinus pinaster	50.64	6.76	41.53	0.00	1.07
Pinus halepensis	48.64	6.84	39.36	0.00	5.16
Erica arborea	52.43	6.98	35.92	0.00	4.67

The experimental device used for the study of the burning behavior is shown in Figure 1. The fuel samples were in the shape of a cylinder with a diameter of 3.5 cm and a mass of 1.5 g. The depth of the sample depended on the bulk densities of the fuel (ranging from 4 to 5 mm). The combustion set-up was composed of a one square meter plate drilled at its centre. A ten square centimeters insulator was included at this location to support the fuel. It was positioned on a load cell in order to measure the fuel mass loss as a function of time. To insure a fast and homogeneous ignition, a small amount of ethanol (0.7 mL) was spread uniformly on the fuel bed and was ignited with a flame torch. An array of 11 thermocouples was positioned above the fuel bed along the flame axis. The first thermocouple was placed 1 cm above the top of the support and the others were located 1 cm from each other. The thermocouples used were mineral-insulated integrally metal-sheathed pre-welded type K (chromel-alumel) pairs of wire with an exposed junction. At the exposed junctions the wires were 50 μm in diameter. The load cell was chosen for its short response time (0.2 s) compared to the analytical balances which have a response time greater than 3 s. The uncertainty in temperature and mass measurements were respectively 0.5 K and 0.031 g. A Schmidt-Boelter gauge (MEDTHERM 64P-02-24T) was used to measure the radiant heat flux emitted from the flame. Its range of sensitivity is from 0 to 0.2 W/cm^2. The radiant heat flux transducer was equipped with a Sapphire window with a view angle of 150 $^\circ$. Based on the manufacturer's data, the standard uncertainty for the measurements was estimated at ± 3 %. The sensor was horizontally oriented and was placed 11 cm from the flame center and at 2.5 cm high. The sampling frequency was 100 Hz for all measurements. Two visible cameras were located inside the room (Figure 1). Camera 1 followed the flame behavior and the flame height. Camera 2 was placed above the flame in order to record the regression of the flame basis. The ambient temperature was 294 K and the relative humidity was 50 %. At least five repetitions were made to collect reliable data for each fuel. An automatic algorithm was developed in order to follow the flame height and the flame radius (recorded by camera 1 and 2 in Figure 1) as a function of time during the combustion. Images were first extracted from videos with a sampling rate of 0.5 Hz as the flame is laminar, axisymmetric and does not flicker. For each image, the flame was segmented from the background by using selection criteria based on the RGB (Red, Green and Blue) components. The first step of the pixel extraction was the selection of pixels with a high magnitude in the red component. In the second step, only the pixels with a certain gap between the red and blue components and the red and green components were kept. Binary images resulting from this processing clearly show the segmented flame.

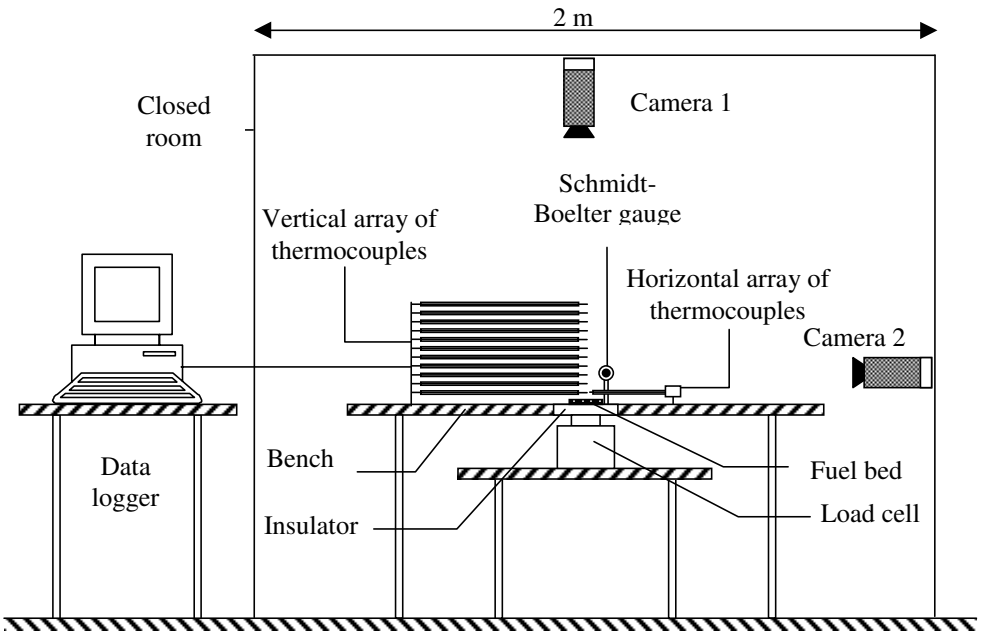

Figure 1. Sketch of the experimental apparatus for the study of the burning behavior.

The composition of the degradation gases was determined thanks to a tube furnace apparatus used as pyrolyser is shown in Figure 2. It is made of a cylindrical furnace 43.5 cm long with an internal diameter of 6.5 cm. The reactor inside, is 86 cm long with an inner diameter of 5 cm. Two thermocouples were used to record the temperature history in the furnace. One was fixed on the inner surface of the furnace and the other was placed in the combustion chamber to follow the temperature in the sample at different heights. Experiments were conducted for the three fuels. Thermogravimetric analysis showed that the most important degradation of the sample occurs between 553 and 703 K (Safi et al., 2004). We chose to study the degradation gases for this range of temperature. The temperature of the furnace was set at 723 K. This furnace temperature allows the samples attaining the chosen range of temperature. Gases were collected into a balloon called the gas sampler, hereafter. The combustion chamber filled with 4 g of sample was kept outside of the furnace until the temperature of the furnace has reached the required value. At the same time, air suction was switched on, the gas sampler was opened and nitrogen was injected at 1 L/min to obtain an inert atmosphere in the device. Once the temperature was stable, the sample was introduced inside the furnace. The injection of nitrogen was stopped, gas sampler was closed and the valve (8a on Figure 2) allowing the ejection of gases outside the apparatus was opened. When samples reached the required temperature, gas sampling began. Valve 8a was closed, a gas sampler was opened and nitrogen was injected into the reactor to fill the gas sampler with pyrolysis gases. Then the gas sampler was directly attached either to the gas chromatograph (Flame Ionization Detector and Thermal Conductivity Detector) or to the hygrometer (EdgeTech Model 2001 Series Dew-Prime) measuring the dew point with a resolution of 0.1 K. The mass loss of the sample between 553 and 703 K was measured for each run. At least three repetitions were carried out. Three tests without fuel were also carried out to verify that there was no leak.

Results and Discussion

The same global tendency was observed for the burning of the all vegetative species, including three different stages (Figures 3 and 4): ignition, laminar flame and extinction. The first stage corresponded to a flickering flame due to the presence of ethanol to ignite the sample. It lasted around 60 s. During the second stage, the ethanol was completely burned and the fuel was only composed of the degradation gases. The flame became laminar. It was absolutely axisymmetric and was slightly conical with a narrow tip. The flame height and radius decreased slowly. The last stage concerned the extinction of the flame.

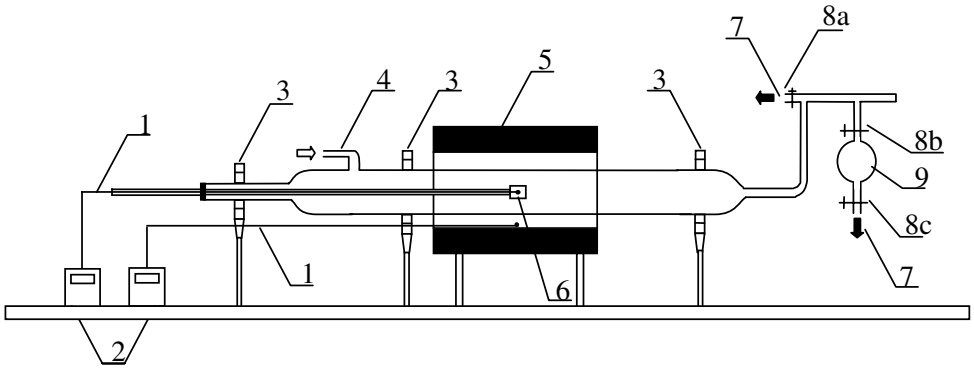

Figure 2. Schematic of the tube furnace (1. thermocouple, 2. temperature controller, 3. bearing, 4. nitrogen injection, 5. electric furnace, 6. combustion boat, 7. air suction, 8a-c. valves, 9. gas samplers).

The remaining solid phase was essentially made up of carbon at the surface of the sample with a certain amount of unburned fuel near the support. Contrary to the other samples, the remaining solid phase of *Erica arborea* was covered by tar.

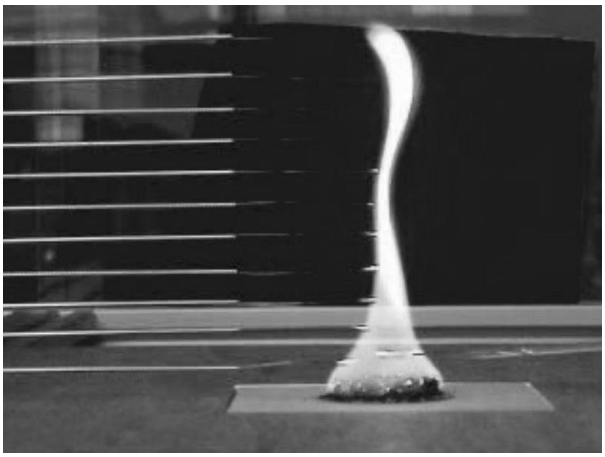

Figure 3. Flame shape during the ignition stage.

The load cell allowed obtaining the evolution of the mass loss for the three samples. The mean mass loss was calculated from five experiments and approximated by 4^{th} order polynomials (Figure 5). At the end of the ignition stage, the mass loss is significant and corresponds to the combustion of ethanol and degradation gases. The global mass loss of the samples is 0.14, 0.21 and 0.25 g respectively for *Pinus pinaster*, *Pinus halepensis* and *Erica arborea*. It corresponds to a percentage between 10 and 18 % of the combustible part of the samples (sample mass minus the ash proportion). During the ignition stage, the less significant mass loss is observed for *Pinus pinaster* whereas the mass loss of the two other species is close. Figure 6 presents the mean mass loss rate for the three fuels during the laminar stage, approximated by 3^{rd} order polynomials. Before 120 s, the mass loss rate of *Pinus halepensis* and *Erica arborea* is roughly the same and *Pinus pinaster*'s one is lower. After 120 s, the mass loss rates of the two pines are close, whereas *Erica arborea*'s one is lower. The extinction of the flame of *Erica arborea* is also quicker than the two other ones.

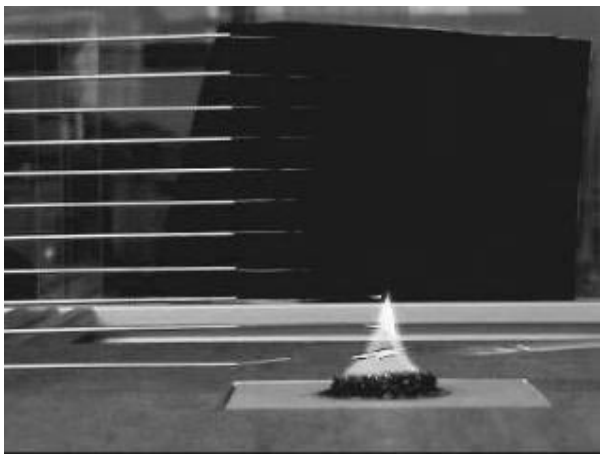

Figure 4. Flame shape during the laminar stage.

The composition of the degradation gases is presented in Table 2. Degradation gases mainly consist of CO_2, CO, CH_4, H_2O, C_4H_6 and lower amounts of C_2 and C_4 hydrocarbons. These results are in agreement with the literature (Grishin et al., 1985). As hemicellulose degrades between 473 and 573 K (White and Dietenberger, 2001), it contributes weakly to the composition of degradation gases occurring during the range of temperature studied here (553 to 703 K). Cellulose is mainly responsible for

the production of flammable volatile gases (LeVan, 1989). Between 573 and 623 K, the formation of tar vapor from cellulose becomes predominant due to the decrease of its degree of polymerization. A deposit of tar on the reactor outside the furnace confirms this result. The degradation of lignin occurs between 498 and 723 K. Although it produces some volatile gases, lignin is mainly responsible for the char formation (Orfão et al., 1999). Thus, the degradation gases come mainly from cellulose (Alén et al., 1996).

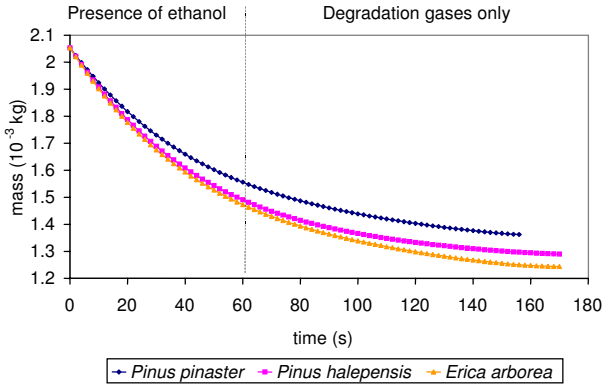

Figure 5. Mean mass loss for the three fuels.

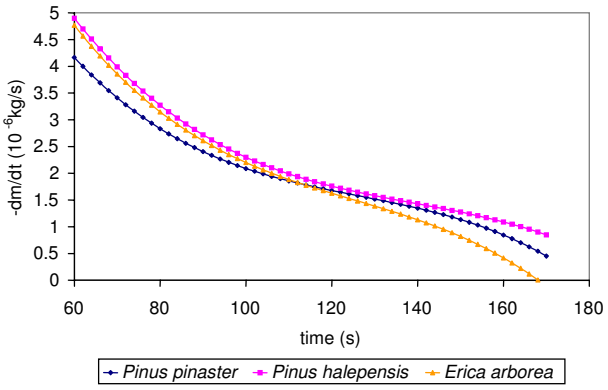

Figure 6. Mean mass loss rate for the three fuels.

The geometrical description of the flame was managed with two visible cameras (Figure 1). Figures 7 and 8 show respectively the flame radius and the flame height versus mass flow rate. For the three species, the radius decrease is slow for high mass flow rate. When the mass flow rate of degradation gases reduces, the regression of the flame base is more significant. The decrease of the flame radius is close for the two pines. For the three fuels, the visible flame height versus the mass flow rate of the degradation gases can be approximated by a straight line.

For *Pinus halepensis*, the slope of the curve changes slightly for heights lower than 1 cm. This part of the graph corresponds to the flame extinction. Contrary to the two other species, the flame extinction of *Pinus halepensis* is more gradual. According to Figure 8, the flame height and the mass flow rate of the degradation gases are also proportional. This observation was made by Jost (1946) too. The highest coefficient of proportionality is obtained for *Pinus pinaster* followed by *Pinus halepensis* and *Erica arborea*. Around 3 10^{-6} kg.s^{-1}, the flames of *Pinus pinaster* and *Erica arborea* have the same mass flow rate and the same flame radius (Figure 7), but have different flame height. The only one parameter that changes between the two fuels is the composition of the degradation gases. Thus, the flame height is mainly proportional to the mass flow rate but depends on the composition of degradation gas.

Table 2. Mass fractions of the pyrolysis gases released by the degradation of the three samples.

	Pinus pinaster	*Pinus halepensis*	*Erica arborea*
CO	0.257	0.205	0.142
CO_2	0.494	0.609	0.722
CH_4	0.078	0.056	0.020
C_2H_4	0.010	0.007	0.004
C_2H_6	0.016	0.010	0.006
C_3H_6	0.001	0.002	0.001
C_3H_8	0.007	0.006	0.005
C_4H_6	0.034	0.023	0.040
C_4H_8	0.011	0.007	0.009
C_4H_{10}	0.003	0.002	0.003
H_2O	0.089	0.070	0.047

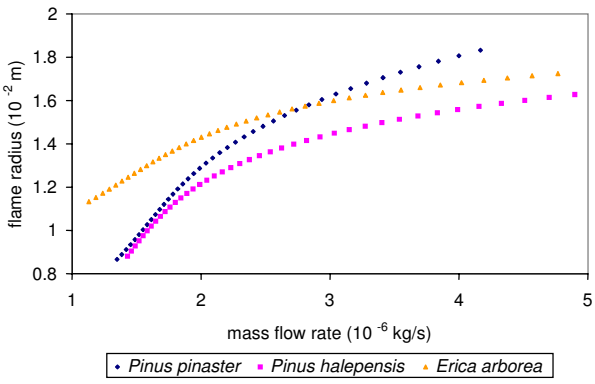

Figure 7. Flame radius versus mass flow rate of degradation gases.

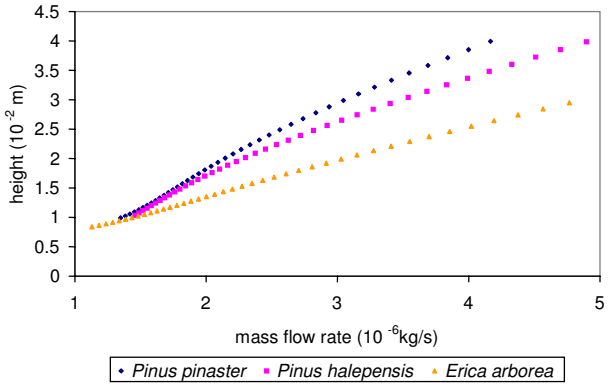

Figure 8. Flame height versus mass flow rate of degradation gases.

The mean time evolution of the radiant heat flux measurement is provided in Figure 9. The highest radiant heat flux occurs during the ignition stage. For the three fuels, the maximum appears about 20 s after the ignition. During the laminar stage, the radiant heat flux decreases slowly up to the flame extinction. The fuel with the greatest heat flux is *Pinus pinaster* followed by *Pinus halepensis* and *Erica arborea.*

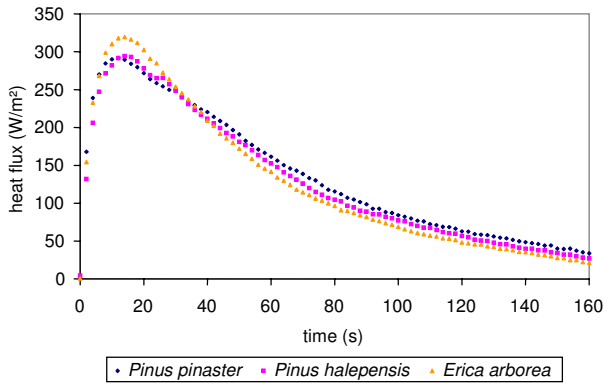

Figure 9. Mean time evolution of the radiant heat flux for the three fuels.

For interpreting the results, the following assumptions have been made: (i) the radiant properties of the heat source are uniform (ii) the rate of radiant energy originates from a point source on the flame axis. This last assumption is available as the distance between the sensor and the flame is higher than three times of the flame diameter (Figure 7). The radiant fraction χ is given by:

$$\chi = \frac{4.\pi.l^2.Q}{\dot{m}.\Delta H} \qquad (1)$$

where l is the distance between the sensor and the flame (11 cm), Q is the radiant heat flux, $\dot{m}$ the mass flow rate and ΔH the low heating value. The low heating values are calculated by means of Dulong's model based on ultimate analysis (Kathiravale et al., 2003), in which the amounts of the elements (C, H, O and S) and the moisture content W are expressed in mass percentages:

$$\begin{aligned}\Delta H(kJ/kg) = \; & 339.13C + 1433.98\,(H - O/8) \\ & +94.20S - 25.12(9H - W)\end{aligned} \qquad (2)$$

According to the Table 1 and with a moisture content of 2 %, the low heating values are 17945, 17752 and 19823 kJ/kg for *Pinus pinaster*, *Pinus halepensis* and *Erica arborea* respectively. According to Figures 6 and 9, the mean radiant fraction over the 60 first seconds of the laminar stage is 0.34 for *Pinus pinaster*, 0.28 for *Pinus halepensis* and 0.22 for *Erica arborea.* Our results are lower than the values found for wood and cellulose (Drysdale, 1985) in literature. The radiant fraction of the flame varies following the fuels. We can suppose that these differences come from the composition of degradation gases released by the forest fuels.

The vertical temperatures follow the same trend for the three species. The mean time evolution of temperature for thermocouples number 1, 2, 3, 4, 5, 7 and 11 are presented in Figure 10 for *Pinus halepensis*, as they are representative of the fire plume. The first stage of the flame (presence of alcohol) lasts approximately 60 s and will not be considered in the following. At the beginning of the second stage, thermocouples 1 to 5 take place inside the laminar flame, while the others (thermocouples 7 and 11) are located above it. The maximum temperature observed in the flame is around 1300 K. As the flame decreases during this stage, thermocouples 1 to 3 remain wrapped up in the flame. Thermocouples 4 and 5 cross the flame during its regression recording successively the temperature of the reaction zone and that of the thermal plume. The temperature decreases progressively from 1100 K to the ambient. The temperature recorded by the upper thermocouples (thermocouples 7 and 11) decrease slowly from 900 K to the ambient with more fluctuations, since the flow becomes progressively turbulent in the thermal plume.

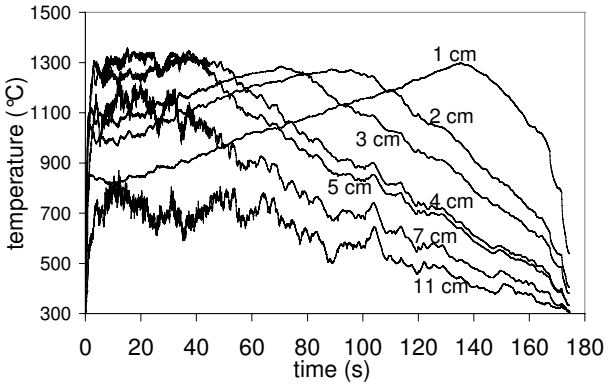

Figure 10. Mean temperatures along the flame axis for *Pinus halepensis.*

Figure 11 presents the time evolution of the mean temperature along the flame axis at 1 cm high for the three fuels during the laminar stage. On this figure, three regions can be distinguished:

- Before 120 s, the thermocouple is in the fuel rich zone where an oxygen deficit appears. When the flame decreases, the reaction zone moves to the thermocouple and the temperature increases steadily.
- Around 130 s, the thermocouple hits the combustion zone. The mean temperature is maximal and is around 1300 K for the three fuels. This similarity can be explained by the heating value per mass of air. It is calculated from the composition of degradation gases (Table 2) and corresponds to the product between the stoechiometric coefficient in air (0.31, 0.42 and 0.59 respectively for *Pinus pinaster*, *Pinus halepensis* and *Erica arborea*) and the reaction enthalpy of degradation gases (10.28, 7.77 and 5.61 $MJ.kg^{-1}$ respectively for *Pinus pinaster*, *Pinus halepensis* and *Erica arborea*). The heating value per mass of air is also 3.23, 3.26 and 3.29 $MJ.kg_{air}^{-1}$ respectively for *Pinus pinaster*, *Pinus halepensis* and *Erica arborea.* Although the reaction enthalpies of the degradation gases are very different, the heating values per mass of air are close for the three fuels as the reaction is piloted by the available dioxygen during the combustion. Thus, the heating values per mass of air are roughly the same for the three fuels and it explains the weak differences of maximal temperature in the flame.
- After 150 s, the thermocouple leaves the reaction zone and is at the beginning of the thermal plume. The temperature decreases progressively from 1100 to 900 K until the flame extinction around 170 s.

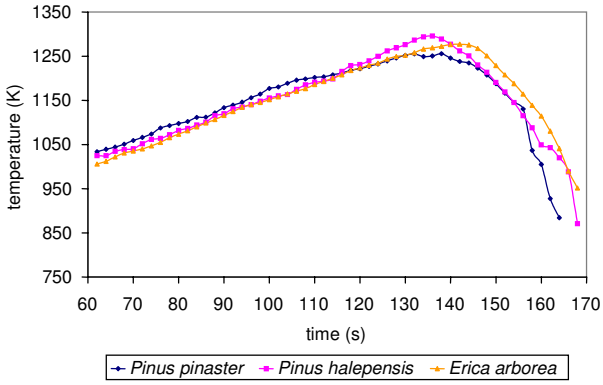

Figure 11. Time evolution of the mean temperature along the flame axis at 1 cm.

To compare the temperature distribution in the flames, it is necessary to keep constant the other parameters (i.e. same mass flow rate and same radius). According to Figure 7, we can only compare the flame of *Pinus pinaster* and *Erica arborea* for a mass flow rate equal to 3 10^{-6} $kg.s^{-1}$. Their curves intersect indeed at this mass flow rate and that, far from the extinction zone (on the left hand side of the figure 7). Figure 12 presents the mean temperatures along the flame axis for *Pinus pinaster* and *Erica arborea.* These temperatures correspond to the mean values around 3 10^{-6} $kg.s^{-1}$ (average on 100 recorded points corresponding to a mass flow rate between 2.97 and 3.03 10^{-6} $kg.s^{-1}$). The two curves have the same maximal temperature but, it does not appear at the same height. For *Pinus pinaster*, the maximum is near 2 cm high whereas *Erica arborea*'s one is at 2.5 cm. We suppose that the combustion of *Pinus pinaster* takes place also closer to the surface sample than *Erica arborea*'s one. This demonstrates that the combustion kinetics depends on the composition of degradation gases. In the thermal plume, the temperature decrease is identical whatever the species. The temperatures are controlled by both radiation losses in the lower part and the mixing of burnt gases with air in the upper part. Thus, in the cooling zone, the curves are only shifted. The differences occurring in this zone are due to the temperature variation of the flame zone.

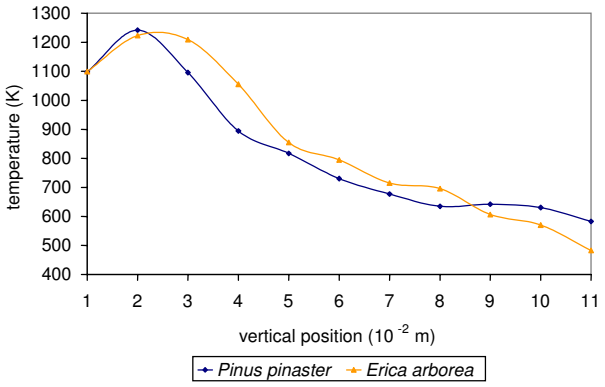

Figure 12. Mean temperatures along the flame axis for *Pinus pinaster* and *Erica arborea.*

Conclusion

In this work, we characterized the degradation gases released by the fuels. We studied the mass loss of the fuel, the flame geometry, the heat flux as well as the temperature distribution. We demonstrated that the understanding of the fire behavior requires also knowledge not only of the solid phase but also of the composition of degradation gases. The main contributions of this work can be summarized as follows:

- Five main gases were identified during the thermal degradation of fuels: CO, CH_4, CO_2, H_2O and C_4H_6.
- The radiant fraction varies also among the species. These differences come from the composition of degradation gases which influences the radiant heat flux emitted by flames.
- The maximal temperature in the flames is roughly the same for the three species as the heating value per mass of air are close.
- The temperature profile obtained experimentally varies among different species mainly in the flame where the combustion kinetics changes following the composition of degradation gases. The differences inside the thermal plume are less significant as the driving phenomena are the radiation losses and the mixing of burnt gases with air.
- The flame height is proportional to the mass flow rate with a non-negligible contribution of degradation gases.

Thus, the whole study confirms that the mass burning rate of the fuel controls the flame dynamics. However, this work shows that the degradation gases must be taken into account for laminar flames to understand the flame behavior. This study provides fundamental data on the flame height, on the maximal temperature and on the heating values per mass of air. These results could be used in models performing the fire behavior at field scale. The preoccupation of the degradation gases appears in multiphase models that describe the gas phase in detail. Our work represents the first step for elaborating a simple and reliable model for gas oxidation, which could be included in two-phases models.

Nomenclature

l	Distance
Q	Radiant heat flux
ΔH	Low heating value
$\dot{m}$	Mass flow rate
χ	Radiant fraction

References

Alén, R., Kuoppala, E. and Oesch, P., "Formation of the main degradation compound groups from wood and its components during pyrolysis", Journal of Analytical and Applied Pyrolysis, 36, 137–148, 1996.

Drysdale, D., An introduction to fire dynamics, Wiley and Sons, 1985.

Dupuy J.L., "Slope and fuel load effects on fire behaviour: Laboratory experiments in pine needles fuel beds", International Journal of Wildland Fire, 5, 153-164, 1995.

Dupuy, J.L., Maréchal, J. and Morvan, D., "Fires from a cylindrical forest burner: combustion dynamics and flame properties", Combustion and Flame, 135, 65-76, 2003.

Ghetti, P., Ricca, L. and Angelini, L., "Thermal analysis of biomass and corresponding pyrolysis products", Fuel 5, 565–573, 1996.

Grishin, A. M., Gruzin, A. D., and Zverev, V. G., "Study of the structure and limits of propagation of the front of an upsteam forest fire", Fizika Goreniya i Vzryva, 21, 11-21, 1985.

Jost, W., Explosion and combustion processes in gases, McGraw-Hill, 1946.

Kathiravale, S., Yunus, M.N.M., Sopian, K., Samsuddin, A.H. and Rahman, R.A., "Modeling the heating value of municipal solid waste", Fuel, 82, 1119-1125, 2003.

Klose, W., Damm, S. and Wiest, W., "Pyrolysis and Activation of Different Woods—Thermal Analysis (TG/EGA) and Formal Kinetics", Forth international Symposium of catalytic and thermochemical conversions of natural organic polymers, Krasnoyarsk, Russia, 9-17, 2000.

LeVan S.L, "Thermal degradation," Concise Encyclopedia of Wood and Woodbased Materials, Pergamon, 271-273, 1989.

Mendes-Lopes, J.M.C, Ventura, J.M.P. and Amaral, J.M.P., "Flame characteristics, temperature-time curves and rate of spread in fires propagating in a bed of pinus pinaster needles", International Journal Wildland Fire, 12, 67-84, 2003.

Orfão, J.J.M Antunes, F.J.A. and Figueiredo, J.L., "Pyrolysis kinetics of lignocellulosic materials – three independent reactions model", Fuel, 78, 349-358, 1999.

Philpot, C.W., "Influence of mineral content on the pyrolysis of plant materials", Forest Science, 16, 461-471, 1970.

Rothermel, R.C. and Anderson, H.E., "Fire spread characteristics determined in the laboratory", USDA Forest Service Research Paper INT-30, 1966.

Saâdaoui, M., Mahjoub Saïd, N., Mhiri, H., Caminat, Ph., Le Palec, G. and Bournot, Ph., "Study of the behaviour of a flame resulting from the combustion of pine needles in a cylindrical basket", International Journal of Thermal Sciences, in press 2007.

Safi, M.J., Mishra, I.M. and Prasad, B., "Global degradation kinetics of pine needles in air", Thermochimica Acta, 412, 155-162, 2004.

Viegas, D.X., "Convective processes in forest fires", Proc. NATO Adv. Study Institute on Buoyant Convective in Geophysical Flows, Kluwer, 401-420, 1998.

White, R.H. and Dietenberger, M.A., "Woods products: Thermal degradation and fire", Encyclopedia of Materials: Science and Technology, 9712-9716, 2001.